uniformity for the screened coil is 6.9% over a cylinder of radius 15 cm which extends ± 10 cm along the z axis. Over the same volume an unscreened Maxwell coil gives a uniformity of 7.8%.

6. Conclusions

We have described a systematic procedure for reducing extraneous magnetic fields outside the active volume of field gradient coil systems. The method can be similarly used for static magnets and RF coils. In NMR imaging, reduction of stray fields in all three types of coil structure is extremely important. The method utilises active magnetic screens and has the advantage that such screens operate independently of frequency down to DC. Some price is paid in terms of reduction of field in the active volume compared with that of the free space value. With time-dependent gradients, the price is in general acceptable since for fast imaging systems employing rapid gradient switching, active coil screening may be the only way in which such imaging schemes may be made to operate in the relatively close confines of an electromagnet.

Acknowledgment

References

Bangert V and Mansfield P 1982 Magnetic field gradient coils for NMR imaging
J. Phys. E: Sci. Instrum. **15** 235–9

Mansfield P and Chapman B 1986 Active magnetic screening of gradient coils in NMR imaging
J. Magn. Res. **66** 573–6

Mansfield P and Morris P G 1982 *NMR Imaging in Biomedicine* (New York: Academic)

A new technique for the real-time recovery of Fabry–Perot line profiles

F J Mulligan
Department of Experimental Physics, St. Patrick's College, Maynooth, Co. Kildare, Ireland

Abstract. A new analogue technique is proposed as a method of obtaining Fabry–Perot line profiles using an imaging photon detector. The technique employs the principle of replacing software with hardware, which increases speed and in this case removes problems due to quantisation errors. A further advantage of the system is that it allows the profile to be observed as the integration proceeds, something which was not possible using the digitised x and y coordinates. The ability to obtain the profile in real-time is of importance when recording from a light source whose intensity varies with time.

1. Introduction

The conventional way to acquire data photoelectrically from a Fabry–Perot interferometer (FPI) has been to scan the wavelength transmitted by the etalon and to monitor the light transmitted through a pin-hole in the centre of the fringe pattern. In the past, FPIs have been classified according to the technique used to effect a wavelength scan. The first of these uses changes with time of the refractive index of the material of the etalon gap caused by changing the pressure. The second method uses change in the etalon spacing effected by piezoelectric drive. Both of the above are usually used in single-channel modes and only temporal scanning is achieved. The third independent variable which controls the wavelength transmitted by the etalon is the angle between the radiation direction and the etalon normal. This variable is the one used in photographic detection, where the spectral elements are scanned spatially rather than in the time-sequential fashion of the spectrometer.

Considerable work has been done in an effort to combine the advantage of the photographic and photoelectric methods (e.g. Shepherd *et al* 1965, Sivjee *et al* 1980, Funfschilling *et al* 1984). The present work uses a prototype, highly light-sensitive, imaging device known as an imaging photon detector (IPD) (Rees *et al* 1980, 1981, McWhirter *et al* 1982) which is described below. A commercial version of this device is available from Instrument Technology Ltd of Hastings, Sussex.

2. The imaging photon detector

The detector employs an S-20 photocathode as the photosensitive element, together with three microchannel plates as the amplifying device; the electron-sensitive element is a linear-resistive anode. Spatial detection on the anode is achieved according to the principles described by Lampton and Carlson (1979) in which the x and y coordinates of the cloud of electrons can be obtained from the signals on the four contact points of the anode. The position of arrival of a photon on the photocathode is registered as a pair of digital x and y coordinates together with a strobe pulse. Each unique pair of coordinates defines a pixel in the computer memory and the

incident image is recorded as a two-dimensional array of photon counts. Figure 1 shows a computer printout of the central fringe in the form of a coded picture, obtained using the experimental arrangement shown in figure 2.
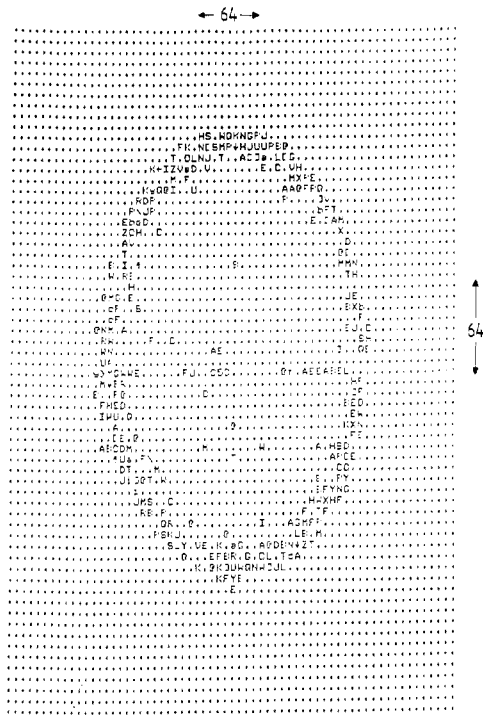

Figure 1. Computer printout of recorded interferogram in the form of a coded picture, showing the central fringe (He–Ne laser suitably attenuated and diffused light source; 30 seconds integration time). The elliptical outline of the processed image is due to the line-printer format.

3. The software aperture

The use of an IPD with a FPI to obtain Doppler shift data on the light source means that the interferogram must be reduced to a plot of intensity versus wavelength. This is achieved by the use of an equal-area annular scan implemented in the software, after the interferogram has been recorded. This method of recovering line profiles is referred to as the 'software aperture' technique. Each annulus represents an equal increment in wavelength, and a plot of the number of counts in each annulus (data point) versus annulus number yields the required spectral profile.

Since the spectral interval recorded by the spectrometer is fixed (determined by the spacing of the F–P plates, the lens focal length and the diameter of the photocathode), the choice of the number of data points in the spectral profile determines the spectral interval per data point. In the present case the number of data points used was 64, which represents a compromise between two conditions:

(*a*) the condition outlined by Zipoy (1979) that the optimum number of sampling points used should be given by the reflectance finesse divided by 2;

(*b*) the condition mentioned by Hays and Roble (1971) that if the number of sampling points is too low, then unwanted harmonics are introduced into the subsequent Fourier analysis.

Figure 3 illustrates the situation for the first few data points in the scan; only pixels whose centres fall within a particular annulus have their counts added to that annulus. Two problems exist with this procedure:

(1) unequal numbers of pixels are included in different annuli, as illustrated in figure 3;

(2) fractions of individual pixels are added to the wrong annuli. This problem becomes much greater at the edge of the interferogram where the spectral interval defined by an individual pixel is considerably greater than that defined by the annulus at that point, as shown in figure 4.

The first problem may be resolved to some extent by normalising the photon count to pixel number for each annulus (Mulligan 1981). Figure 5 illustrates the result of such a normalisation for a He–Ne laser fringe. At the edge of the recorded spectrum, normalisation does not work very well on account of the reduced sensitivity at the edge of the detector. The obvious solution to both problems is to choose a sufficiently small pixel size; pixel size is limited by the amount of memory space available in the computer and the electronic performance of the resistive anode. In the present case, the number of pixels used is 64×64 (figure 1) with a maximum count per pixel of
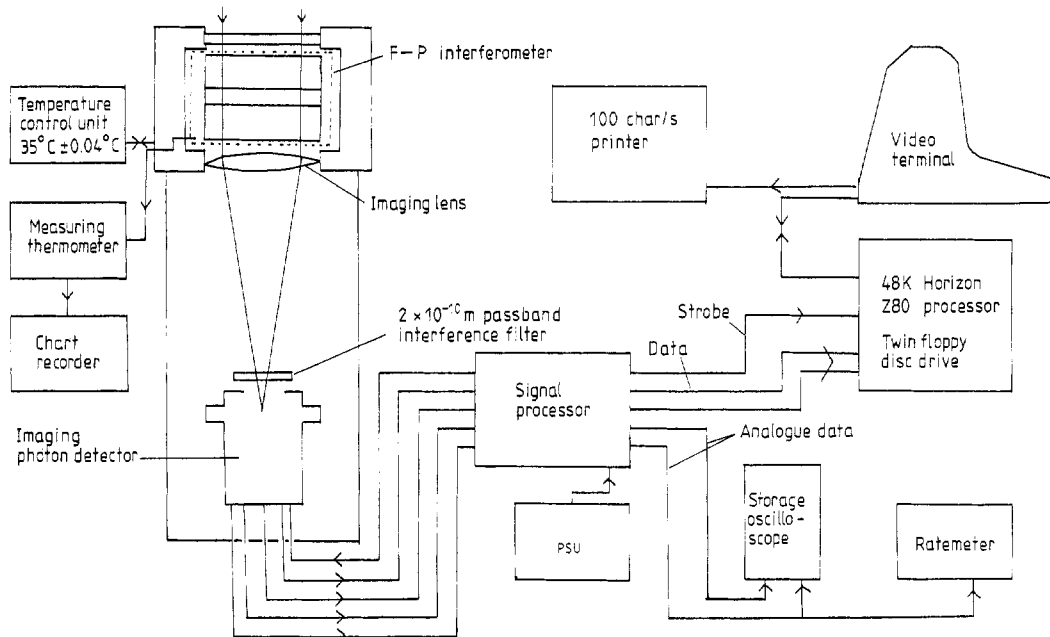

Figure 2. Schematic diagram of Fabry–Perot interferometer.
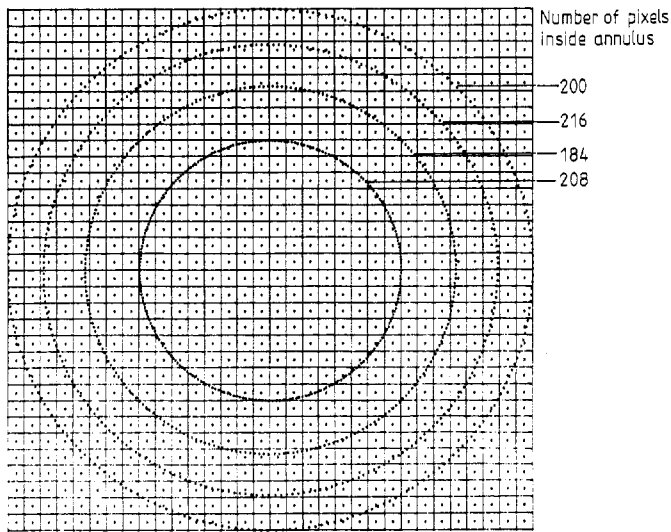
Figure 3. Software aperture showing different numbers of pixels in different annuli.

65 535. Figure 4 shows that this resolution is not sufficient to obtain an ideal profile at the edge of the interferogram.

An alternative approach is to perform the radius-squared reduction (annular scan) as the data is arriving. This has the advantage that memory space limitations are removed, but the deadtime of the counting system is considerably increased due to the need to calculate the distance of each photon arrival from the fringe centre.

4. Analogue pre-processing

The two problems mentioned above are inherent to the recovery of data due to quantisation errors in the digitisation process. One way to avoid both problems is to calculate the radius-squared values in an analogue way, and then to perform the digitisation on the radius-squared values necessary for recording the data in a computer. The x and y coordinates are available before digitisation as analogue signals in the range 0 to +10 V, representing the full spatial range of the detector. These two signals can be fed to an oscilloscope in the XY-mode for a visual inspection of the data; figure 6 is a photograph of a typical oscilloscope trace. Approximate values of the x and y coordinates of the centre of the fringe system (C_x, C_y) may be
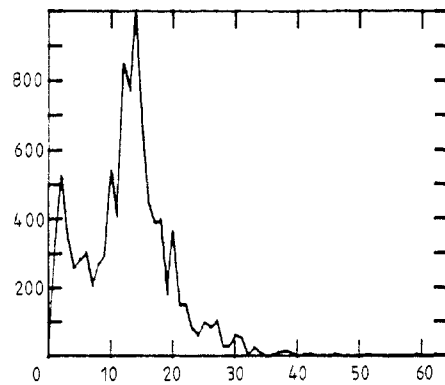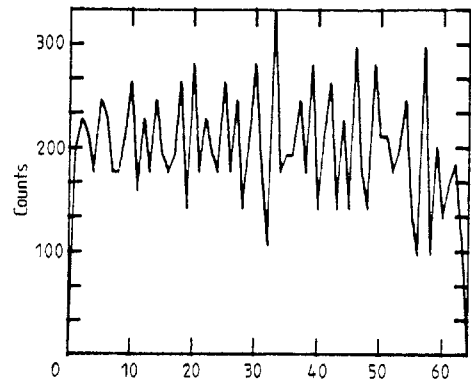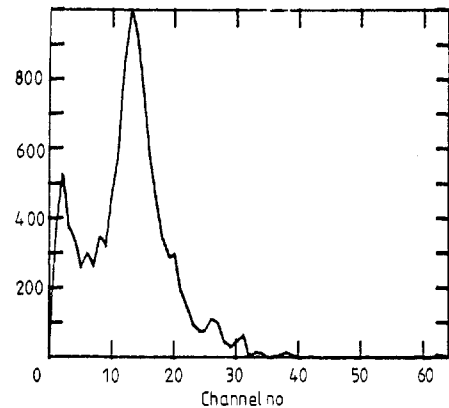

Figure 5. Result of normalising the recorded profile to pixel number. (*a*) un-normalised profile, (*b*) normalisation profile, (*c*) normalised profile.
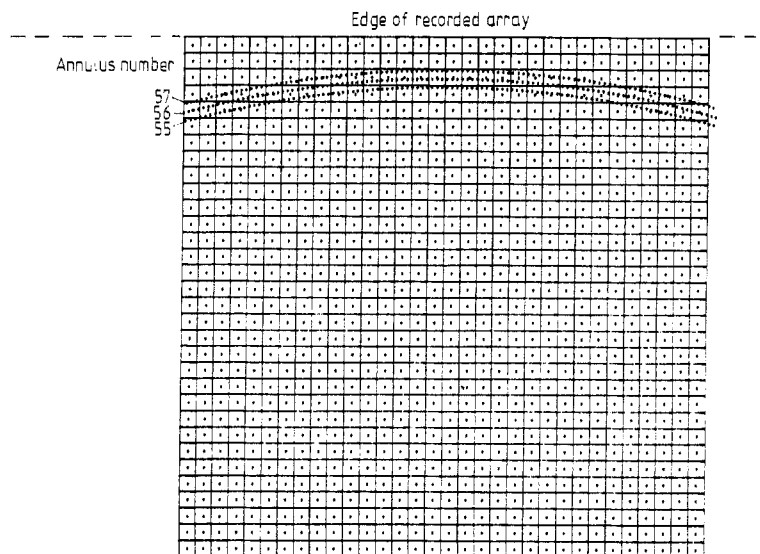

Figure 4. Comparison of relative size of pixel to annulus at edge of recorded interferogram.

obtained from the oscilloscope. The values of the centre coordinates are used to transform the fringe system so that the centre of the pattern corresponds to the coordinates (0 V, 0 V); i.e. C_x is subtracted from all x coordinates and C_y is subtracted from all y coordinates. The x and y coordinates now range approximately from -5 V to $+5$ V. Next the values $(x-C_x)^2/10$ and $(y-C_y)^2/10$ are calculated using two AD533 analogue multipliers. Finally the sum of the two terms above is obtained and multiplied by 2 to yield a value of radius-squared which has a full range (0 to $+10$ V); figure 7 is a schematic diagram of the circuitry used.
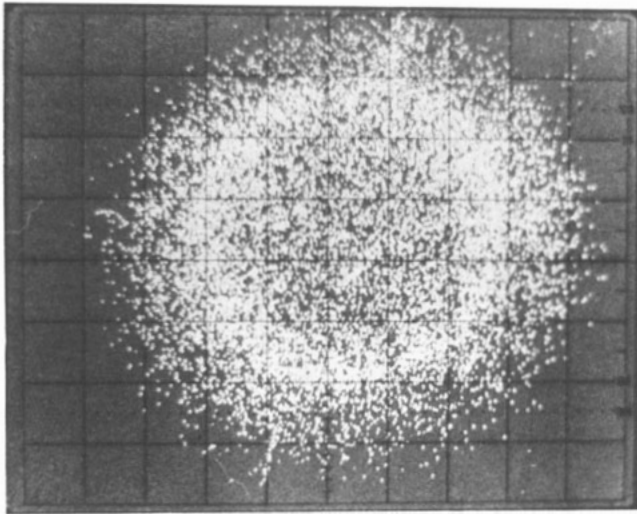

Figure 6. Photograph of central fringe on oscilloscope using He–Ne laser as light source (integration time 4 seconds).

Each detected photon now has a radius-squared value associated with it. These values are fed to a pulse-height analyser and the resulting profile represents a plot of recorded photon number (intensity) versus radius-squared (wavelength). The x and y inputs to the analogue circuitry are the outputs from two sample-and-hold gates, and the resulting values of R^2 are held until the next pair of x and y values arrive. In this mode of operation, it is necessary to strobe the data into the pulse-height analyser (i.e. the pulse-height analyser only samples the incoming R^2 signal on the arrival of the strobe). The strobe is already available for use with the software aperture system, but it must be delayed by a few microseconds due to propagation delay of the signals through the analogue pre-processing circuitry.

Since the centre coordinates used to obtain the profile are only approximate values read from the oscilloscope, they need to be adjusted; this is achieved using two externally available multiturn potentiometers. During successive integrations; the x and y centre coordinates (C_x, C_y) are alternately adjusted to obtain the 'best' coordinates as determined by the half-width of the line profile.

5. Performance

Figures 8(a) and (b) show the same laser profile recorded using the software aperture technique and the pre-processing method respectively; the profiles were recorded simultaneously and equal integration times were used (60 seconds). The combination of a large dark signal, together with the reduced response of the detector with increasing radius from the centre, account for the asymmetrical nature of both profiles. Figures 9(a) and (b) show the response of the detector when illuminated uniformly across its diameter. The dark count was 400 count/s with a signal count of 800 count/s at a temperature of 20 °C – high dark count rates are a feature of IPDs with linear-resistive anodes (Lampton and Carlson 1979). The rapid decrease in sensitivity to near zero after only about 30 channels may be explained by referring initially to the software aperture system. Approximately 9 pixels all around the perimeter of the 64 × 64 array are not used, due to the fact that the full range of the analogue-to-digital converters (ADCs), used to provide the digital x and y coordinates, is not being exploited; this is confirmed by pulse-height analysis of the signals going to the ADCs. It is possible to adjust the gain of the amplifiers before the ADCs so that the full range is used, but as will be shown below, it is not necessary to make this adjustment and this facility would not normally be available to the end-user.
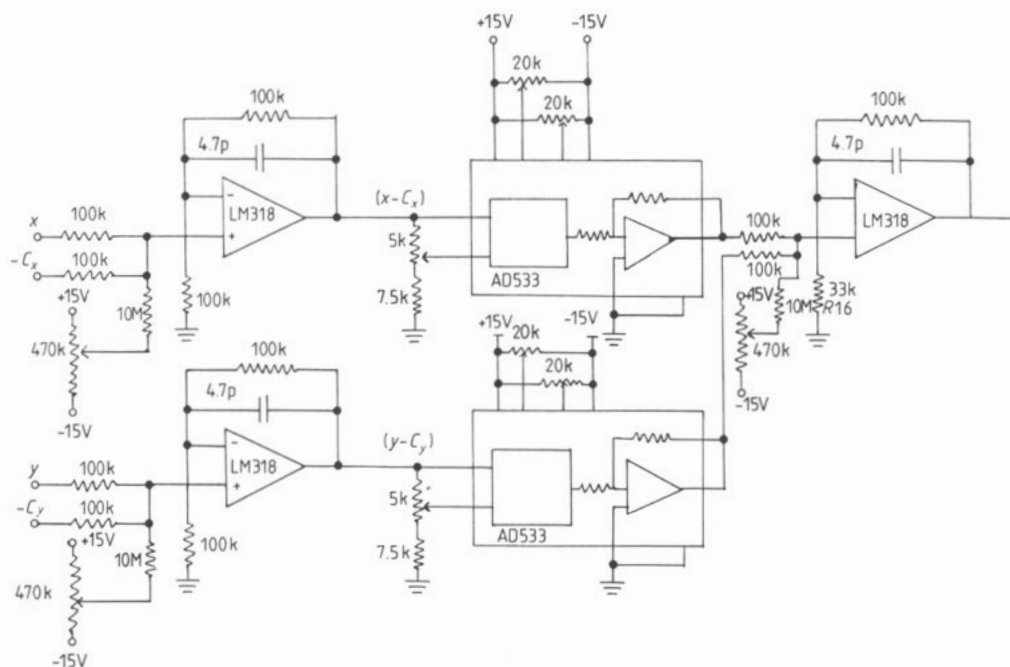

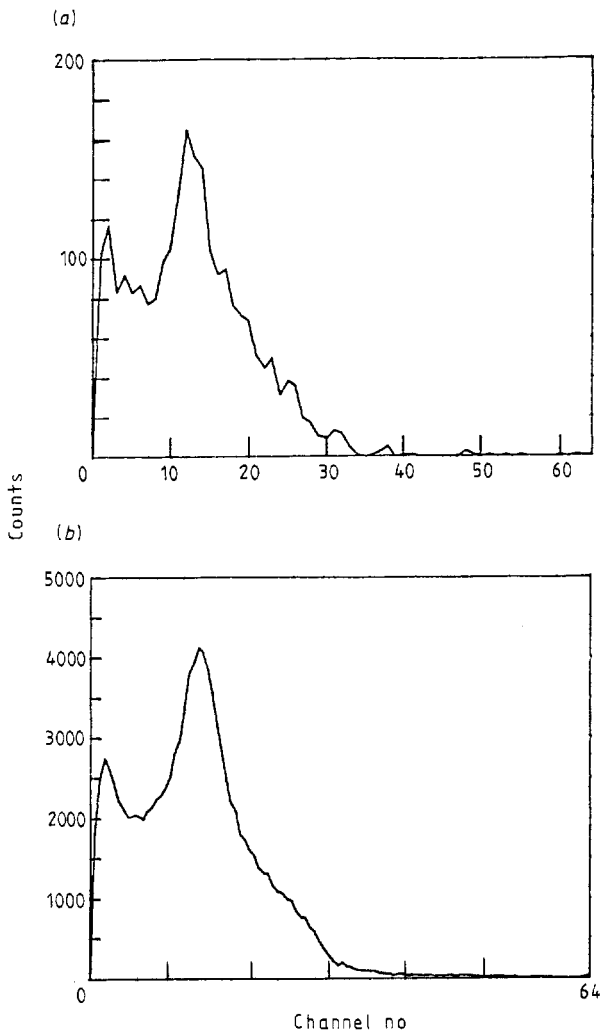**Figure 7.** Pre-processing electronics.

Figure 8. (*a*) He–Ne laser line profile recorded using software aperture system. (*b*) He–Ne laser profile recorded using analogue pre-processing circuitry with pulse-height analyser.

Figure 9. Profiles obtained from software aperture system (*a*), and analogue pre-processing system (*b*), when photocathode is illuminated uniformly.

When the 64 × 64 array is transferred to *R*-squared space to produce the line-profile, the 9 pixels on the perimeter become 30 channels in *R*-squared space. Figure 10 shows a section of the
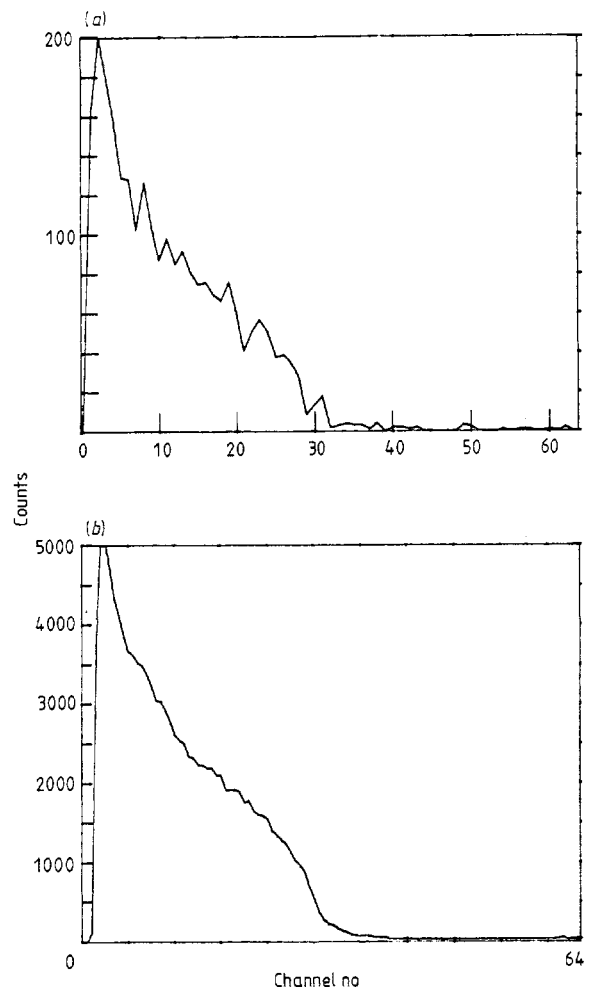
software aperture on the two-dimensional array, which illustrates this point. As has been mentioned above, it is not necessary to adjust the gain of the amplifiers before the ADCs; if the 64 channels are taken from the active area as shown in figure 11, then a plot of this profile yields a much more acceptable
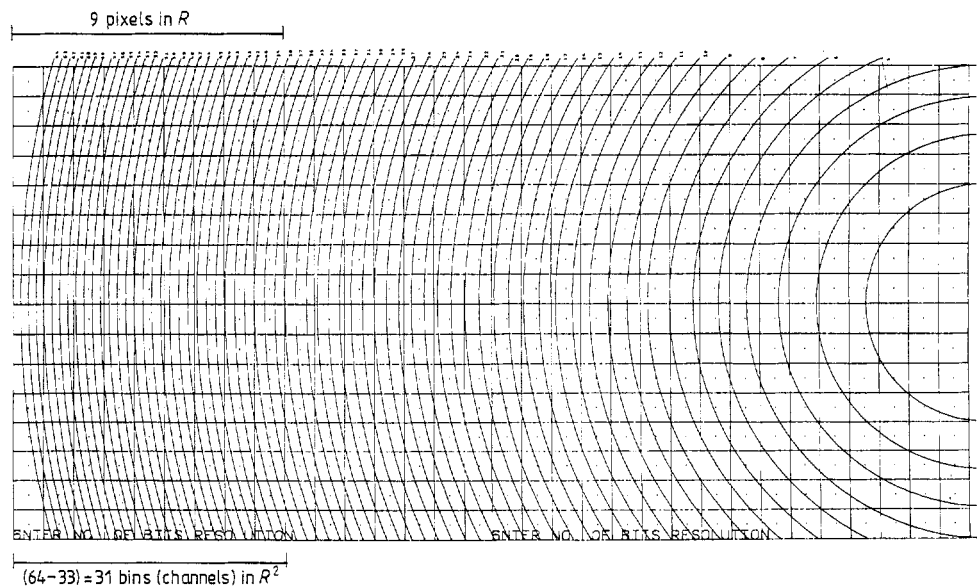

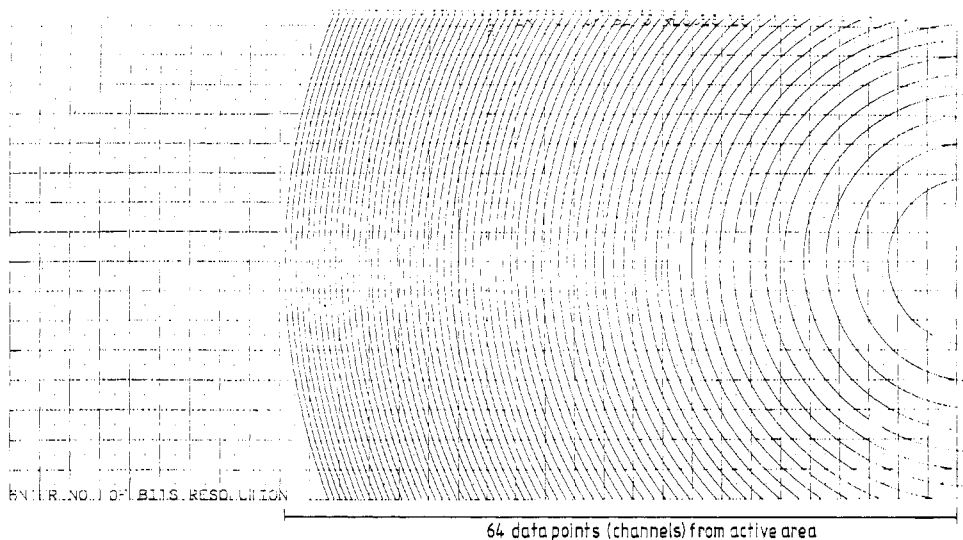**Figure 10.** Section of software aperture on 64 × 64 array.

Figure 11. Section of software aperture on active area of 64 × 64 array.

performance trace as shown in figure 12. The aperture can be quite easily changed by simply changing the R-squared array, and is thus well named as a 'software aperture'. The limitation on how far one can continue this process is determined by the inherent limitations of resolution of the detector itself, which according to Rees *et al* (1980) is about 100 μm for a gain of 10^7. In the case of the analogue pre-processing system, simply adjusting the gain of the final output amplifier, i.e. $R16$ in figure 7, has the same effect as changing the software aperture. Increasing the gain spreads out the profile more and the result is that the 64 data points may be taken from the active area of the IPD.
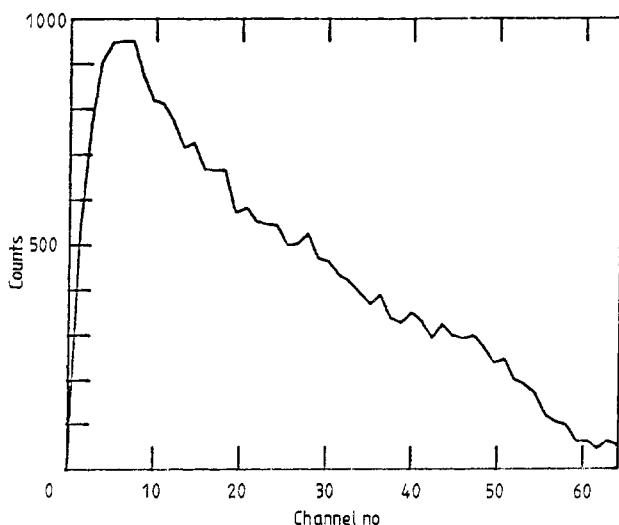

Figure 12. R-squared performance profile resulting from software aperture as shown in figure 11, when photocathode is illuminated uniformly.

The maximum processing rate of the analogue system is about 200 kHz, limited initially by the AD533 squarers. This is far in excess of any possible signal as the IPD begins to be degraded if count rates exceed 10 kHz. At a rate of 2000 count/s the software aperture system detects only about 1/60th of the counts recorded by the analogue technique, and

the corresponding increase in signal-to-noise ratio is apparent from figures 8(*a*) and (*b*). A further advantage of the new system is that the profile may be observed as the integration proceeds, something which was not possible with the software method.

The disadvantage of replacing the software aperture method by analogue pre-processing is that DC drift is now a greater possible source of error. Comparison of measured values of R^2 with calculated values showed that the overall error of the electronics was less than $\pm 2\%$, with the greatest error for values of R^2 less than 1 V. When the two profiles are superimposed, a slight broadening in the new system profile is apparent. The specifications of the AD533 analogue multiplier indicate a maximum error of $\pm 1\%$. An improvement in the circuitry may be obtained by replacing the AD533 by the internally laser-trimmed AD534, which has a maximum error of $\pm 0.25\%$.

The new system is particularly sensitive to changes in the centre coordinates, C_x and C_y, which are adjusted to a resolution of 0.01 V. This corresponds to a distance of 30 μm on the photocathode surface, whereas the theoretical resolution of the IPD is only 300 μm (Rees *et al* 1980). In the software aperture system the centre coordinates are adjusted to 150 μm.

6. Conclusions

The analogue pre-processing method eliminates errors present in an earlier system due to quantisation in the analogue-to-digital converters. The system is more sensitive and a significant increase in the signal-to-noise ratio is obtained over the software aperture method. Profiles may be obtained in real-time, but a slight broadening of the recorded profile is introduced due to errors in the analogue computation.

References

Funfschilling J, Brulhart M, Hidber H R and Zschokke-Granacher I 1984 Optical multichannel detection system suitable for a Fabry–Perot interferometer
Rev. Sci. Instrum. **55** 153–7

Hays P B and Roble R G 1971 A technique for recovering Doppler line profiles from Fabry–Perot interferometer fringes of very low intensity
Appl. Opt. **10** 193–200

Lampton M and Carlson C W 1979 Low-distortion resistive anodes for two dimensional position-sensitive MCP systems
Rev. Sci. Instrum. **50** 1093–8

McWhirter I, Rees D and Greenway A H 1982 Miniature imaging photon detectors III. An assessment of the performance of the resistive anode IPD
J. Phys. E: Sci. Instrum. **15** 145–50

Mulligan F J 1981 Interferometric wind and temperature measurements in the thermosphere
Thesis St. Patrick's College, Maynooth, Ireland

Rees D, McWhirter I, Rounce P A, Barlow F E and Kellock S J 1980 Miniature imaging photon detectors
J. Phys. E: Sci. Instrum. **13** 763–70

Rees D, McWhirter I, Rounce P A and Barlow F E 1981 Miniature imaging photon detectors II. Devices with transparent photocathodes
J. Phys. E: Sci. Instrum. **14** 229–33

Shepherd G G, Lake C W, Miiller J R and Cogger L L 1965 A spatial spectral scanning technique for the Fabry–Perot spectrometer
Appl. Opt. **4** 267–72

Sivjee G G, Hallinan T J and Swenson G R 1980 Fabry–Perot-interferometer imaging system for thermospheric temperature and wind measurements
Appl. Opt. **19** 2206–9

Zipoy D M 1979 Fabry–Perot inversion algorithm
Appl. Opt. **18** 1988–95

Isotope shift measurements with polarised light

P Aufmuth, K Heilig and K-D Körwers†
Institut für Atom- und Molekülphysik, Abteilung Spektroskopie, Universität Hannover, 3000 Hannover 1, Federal Republic of Germany

Abstract. A new device for measuring isotope shifts using a photoelectric recording Fabry–Perot spectrometer is described. The light beams of two fixed hollow cathodes are combined by means of a Wollaston prism to follow a common path through the spectrometer and then the two beams are separated by another Wollaston prism. This instrument allows measurements to be made with the same degree of accuracy as conventional set-ups, but is easier to handle and offers the additional advantage of allowing the simultaneous investigation of two light beams.

1. Introduction

The analysis of optical spectra is an important method of studying atoms and molecules. The finer details of these spectra (hyperfine structure and isotope shift) give information on the properties of electron shells and nuclei. This article deals with isotope shift measurements.

To perform isotope shift measurements a hollow cathode is often used (Hansen *et al* 1967). This is a reliable and universal light source. Customarily one uses several stand-by hollow cathodes (one for each isotope) arranged in the form of a 'roundabout'. While measuring, each new hollow cathode has to be brought rather quickly into exactly the same position, in the ray path of the spectrometer, as the last one. To overcome the problems of adjustment and reproducibility of such a device, we have constructed an arrangement with fixed hollow cathodes.

In § 2 we describe the problems encountered with conventional set-ups and in § 3 and 4 the new device. After reporting results of test performances (§ 5), we give a general discussion of further applications in § 6.

2. Conventional set-up

In almost any atomic spectral line the following isotopic effect appears: each even isotope of an element contributes to the spectral line (corresponding to a certain electronic transition) with a wavenumber slightly different from the other isotopes' wavenumbers. This contribution, called a 'component', is Doppler broadened. The difference in wavenumber of the components is the isotope shift. (In the case of odd isotopes the hyperfine interaction leads to more than one component and one has to consider the centre-of-gravity of this splitting.) In many cases the isotope shift is smaller than the Doppler width. Then, not only one but a number of light sources is used—one highly enriched isotope per light source.

Conveniently hollow cathode lamps serve to excite the atomic or ionic spectra. To measure the shift between two isotopes the different hollow cathodes are brought alternately

† Present address: Digital Equipment GmbH, Freischützstrasse 91, 8000 München 81, Federal Republic of Germany.